Modal analysis of noise in signal-processing-in-the-element detectors

Frank J. Effenberger and Glenn D. Boreman

Detector noise limits the performance of signal-processing-in-the-element detectors. For detectors to be optimized, an expression for the signal and noise must be found. The results of the eigenmode solution to the charge transport problem are used to derive the power spectral density of the noise in analytic form. This result is then coordinated with a similarly obtained modulation transfer function to yield a frequency-dependent signal-to-noise ratio (SNR). The SNR is used to reveal performance trends over several ranges of detector parameters. The most important result is that the contact boundary velocity strongly controls the SNR. The optimum SNR condition occurs when the contacts are not perfectly ohmic but exhibit a partially blocking behavior.

Key words: Signal processing in the element, infrared detectors, charge transport, noise power spectral density.

1. Introduction

In any detector system, the fundamental limitation on total performance is the noise generated in the detector itself. For this reason, a complete description of the noise intrinsic to the detector is essential for predicting system capabilities. In most cases, the noise in detectors can be considered a wide-sense stationary, ergodic process. When this is true, the noise can be described adequately by an average value and an autocorrelation function, or conversely by a power spectral density (PSD). If the PSD is known, a host of useful performance criteria, such as signal-to-noise ratio (SNR), noise-equivalent power, and detectivity (D^*) can be computed. Thus an accurate determination of the noise PSD is an important step in device characterization.

Signal-processing-in-the-element (SPRITE) detectors[1] improve the SNR over simpler photoconductive detectors by implementing a time-delay-and-integration process internal to the detector element. Drift transport of carriers through the detector, in conjunction with a scanned input image, causes this to occur. Unfortunately, recombination and diffusion degrade detector performance by removing and spreading the detected charge, respectively. These imperfections affect not only the signal but also the noise generated in the detector. Thus, for the noise output of a SPRITE to be understood fully, a correct analysis of the charge transport is necessary.

In previous analyses,[2–4] a one-dimensional free-space Green's function was taken as the solution to the transport equation. This solution includes diffusion, which tends to smooth the charge distribution; drift, which moves the charge along the length of the device; and recombination, which reduces the signal level over time. This solution, which describes the charge distribution in an infinite one-dimensional solid resulting from a point source, is used as the basis of calculations to compute the transfer of a scanned incident-radiation distribution on the SPRITE detector bar into a output voltage across the readout terminals.

To derive an expression for the noise PSD, the above analyses use a Green's function to derive the response at the readout resulting from a point source at an arbitrary position on the detector. Then, through the use of the assumption that noise generation in the detector material is uncorrelated from point to point and time to time, the total noise spectrum is found by integration of the squared magnitude of the point response over the entire length of the detector. This gives a result that resembles a simple low-pass filter characteristic, with a flat power density at zero frequency and a roll-off at the frequency corresponding to the inverse of the carrier lifetime.

The authors are with the Center for Research and Education in Optics and Lasers, Department of Electrical and Computer Engineering, University of Central Florida, Orlando, Florida 32816.

Received 2 December 1994; revised manuscript received 25 July 1995.

0003-6935/96/040566-06$06.00/0

This theory does not give complete agreement with the measurements of real devices.[5] The theory provides only a qualitative description of the signal-to-noise improvement caused by the time-delay-and-integration function intrinsic to the SPRITE detector. Of particular interest is the behavior of actual devices at low frequencies. As mentioned above, the Green's function analysis predicts a flat PSD at low frequencies. What is actually observed is a substantial $1/f$ behavior.[6] Although this behavior may be caused by a number of effects, such as poor contacts or thermal fluctuations, no attempt has yet been made to investigate theoretically this $1/f$ PSD characteristic.

As discussed in our previous paper,[7] a method for analyzing the transport in a SPRITE detector was developed by the use of a modal decomposition of the carrier density in the detector structure. This analysis is more complete than the Green's function method in that the three-dimensional nature of the SPRITE is addressed, as well as the effect of arbitrary boundary conditions. Although it should be noted that previous analyses have addressed boundary effects, these studies still use the basic Green's function solution. As stated above, this solution is intrinsically a free-space model. The method of Ref. 7, a separation of variables followed by the determination of eigenmodes, implicitly incorporates the effects of the boundaries by generating the set of charge-density modes in the detector that satisfy the boundary conditions. These modes were used to decompose an impulsive scanned input and to reconstruct the resultant output.

Here we use the same modal analysis as the basis for a study of the noise PSD. Section 2 discusses the several assumptions made about the nature of the noise-generating processes. An expression for the noise PSD is then derived. In Section 4, the PSD and modulation transfer function (MTF) results are combined to produce the frequency-dependent SNR. Finally, the SNR curves are used as a means of comparison to optimize several detector parameters.

2. Noise Transport Problem

This section addresses the assumptions made about the noise sources in an idealized SPRITE detector. The first assumption is that the noise can be described as a random charge input at each point in the detector. It is assumed that this random signal is uncorrelated from point to point and from time to time. This implies that the PSD of this generation signal contains all the frequencies (white noise), and that the signals from two different points in the detector will add in quadrature. These assumptions were used by Shepherd and Day[2,3] and are generally applicable to SPRITE detectors.

However, the noise input being uncorrelated in space does not imply that the noise charge will be uncorrelated in space. The noise input is filtered by the processes of drift and diffusion to result in the noise charge distribution.[8] As seen in Section 3, the consequence of this processing is that the PSD of the noise is no longer white.

It is also assumed in part of the derivation that the local spatial intensity of the noise is constant over the detector. If we assume that the dominant noise source is generation-recombination noise, then the noise charge intensity will depend on the minority carrier densities. Because of carrier drift this density does not remain constant over the length of the detector. Indeed, this nonuniformity in carrier density causes a variation in drift speed along the bar because of background integration.

An estimate of the noise nonuniformity can be found if we assume that the excess carriers are only drifting, and not diffusing or interacting with the boundaries. This assumption implies that the time, t_B, a given population of carriers, $\rho(z_B, t_B)$, in the SPRITE has been directly proportional to the distance from the beginning of the bar, z_B. Thus we can write $t_B = z_B/V$, where V is the drift velocity. Because no diffusion or boundary conditions exist, the population at any place and time does not interact with the neighboring populations. Thus we can describe the excess carrier population with a simple, spatially independent generation-recombination equation, such as

$$\frac{\mathrm{d}\rho}{\mathrm{d}t_B} = G - \frac{\rho}{\tau}. \tag{1}$$

This has the solution

$$\rho(z_B, t_B) = 1 - \exp\left(-\frac{t_B}{\tau}\right) = 1 - \exp\left(-\frac{z_B}{V\tau}\right). \tag{2}$$

The noise power from either generation or recombination is proportional to the rate at which these processes occur. The generation rate is a constant, G, and so the generation noise is constant. The recombination rate is equal to $\rho(z_B)/\tau$, which is not constant over the length. These two noise powers add independently, and thus they give the following charge noise amplitude $\sigma_N(z_B)$:

$$\sigma_N(z_B) = \left[2 - \exp\left(-\frac{z_B}{V\tau}\right)\right]^{1/2}. \tag{3}$$

The variation in this noise amplitude has a total variation of approximately 30% of its maximum level. For this reason, the assumption of constant charge noise amplitude is made. This is not required for the following analysis to be valid; however, it does simplify the calculation.

3. Noise Power Spectral Density

Given the above assumptions, we now derive the noise PSD of a SPRITE detector, using the theory, terminology, and symbology of Ref. 7. This formal-

ism is used to model the effects of the random noise inputs to the SPRITE detector. The final result is an analytical expression for the noise PSD. The PSD is pivotal to the characterization of the noise in that it permits computation of noise power for any given frequency band of interest. Here we begin by computing the response to a point-impulse input.

An input impulse point charge source located at a point (x_0', y_0', z_0'), occurring at $t = 0$, with a strength f, denoted $q(x', y', z', t')$, can be written as

$$q_i(x', y', z', t') = \delta(x' - x_0')\delta(y' - y_0') \times \delta(z' - z_0')\delta(t')f(x_0', y_0', z_0'). \quad (4)$$

Here we have allowed the strength of the point source to vary from point to point. We must first decompose this point-impulse input into the modes of the structure,

$$q_i(x', y', z', t') = \sum_{p,q,r} c_{pqr}X_p(x')Y_q(y')Z_r(z') \times T(t')\exp(N_{dz}z'), \quad (5)$$

where X_p, Y_q, and Z_r denote the spatial profiles of the modes. We can find the modal amplitudes, c_{pqr}, by using the property that the solutions are orthogonal when integrated over the domain of the detector, yielding

$$c_{pqr} = \frac{\iiint \mathrm{d}x'\mathrm{d}y'\mathrm{d}z' X_p(x')Y_q(y')Z_r(z')\exp(-N_{dz}z')q_i(x', y', z', t')}{\iiint \mathrm{d}x'\mathrm{d}y'\mathrm{d}z' X_p^2(x')Y_q^2(y')Z_r^2(z')}. \quad (6)$$

Performing the indicated integrations, we arrive at

$$c_{pqr} = \frac{\cos[k_{xp}x_0' + p(\pi/2)]\cos[k_{yq}y_0' + q(\pi/2)]\exp(-N_{dz}z_0')\cos[k_{zr}z_0' + r(\pi/2)]}{[1 + |\mathrm{sinc}(2k_{xp})|][1 + |\mathrm{sinc}(2k_{yq})|][1 + |\mathrm{sinc}(2k_{zr})|]} f(x_0', y_0', z_0'). \quad (7)$$

We now take the modal amplitudes and compute the output readout charge, $Q(t', x_0', y_0', z_0')$. We can use the same mode-to-output constants, b_{pqr}, derived for the MTF calculation [Ref. 7, Eq. (27)] to write

$$Q(t', x_0', y_0', z_0') = \sum_{p,q,r} c_{pqr}u(t')\exp(-k_{pqr}^2 t')b_{pqr}. \quad (8)$$

The output spectrum is found by taking the Fourier transform of this impulse response:

$$\overline{Q}(\omega', x_0', y_0', z_0') = \mathcal{F}[Q] = \sum_{p,q,r} c_{pqr}b_{pqr}\frac{1}{k_{pqr}^2 + j\omega'}. \quad (9)$$

This transform of the point-impulse response is the point transfer function of the SPRITE. This differs from the scanned MTF result relevant to the analysis of the signal in the SPRITE detector. The scanned MTF describes the spectral filtering that operates on a line input of light that is being scanned across the length of the detector at the drift speed of the carriers. The point MTF of Eq. (9) describes the spectral filtering that operates on a spatial and temporal impulse of light that occurs at a specific location in the detector.

We relate this point transfer function to the total PSD by using the assumption that the SPRITE transport process is linear. The PSD of the output caused by noise at point (x_0', y_0', z_0'), $\mathrm{PSD}_{\mathrm{OUT}}$, is related to the input PSD of the noise at that point, $\mathrm{PSD}_{\mathrm{IN}}$, by the squared magnitude of the transfer function, thus

$$\mathrm{PSD}_{\mathrm{OUT}}(\omega', x_0', y_0', z_0') = \overline{Q}^*(\omega', x_0', y_0', z_0')\overline{Q}(\omega', x_0', y_0', z_0') \times \mathrm{PSD}_{\mathrm{IN}}(\omega', x_0', y_0', z_0'). \quad (10)$$

At this point we can use the fact that $\mathrm{PSD}_{\mathrm{IN}}$ is constant (i.e., white). Multiplication of the transfer function with its complex conjugate requires the reexpression of one set of infinite sums by replacement of the old indices, p, q, r, with new indices, α, β, γ. This results in the following six-dimensional sum for the output PSD resulting from a noise input at (x_0', y_0', z_0'):

$$\mathrm{PSD}_{\mathrm{OUT}}(\omega', x_0', y_0', z_0') = \sum_{p,q,r}\sum_{\alpha,\beta,\gamma} \frac{b_{pqr}b_{\alpha\beta\gamma}c_{pqr}c_{\alpha\beta\gamma}}{(k_{pqr}^2 + j\omega)(k_{\alpha\beta\gamma}^2 - j\omega)}. \quad (11)$$

To obtain the total PSD, S_N, resulting from noise over the entire detector, we sum the contributions of each point. To do this, we must assume that the noise inputs are uncorrelated from point to point in the detector. Because of this, the noise amplitudes add in quadrature, and therefore the power spectral

densities add arithmetically. Because our noise inputs are infinitesimal, this requires integration over the entire detector; thus

$$S_N(\omega') = \int_{-1}^{1}\int\int \mathrm{d}x_0'\mathrm{d}y_0'z_0'\mathrm{PSD}_{\mathrm{OUT}}(\omega', x_0', y_0', z'). \quad (12)$$

This integral can be simplified because orthogonal properties of the eigenmodes cause the terms where $p \neq \alpha$ and $q \neq \beta$ to integrate to zero. This eliminates two of the six indices of Eq. (11), producing the following expression for the PSD:

$$S_N(\omega') = \sum_{p,q,r,\gamma} \frac{b_{pqr}b_{pq\gamma}a_{r\gamma}}{[1 + |\mathrm{sinc}(2k_{xp})|][1 + |\mathrm{sinc}(2k_{yq})|](k_{pqr}^2 + j\omega)(k_{pq\gamma}^2 - j\omega)}. \quad (13)$$

We have defined a new set of constants, $a_{r\gamma}$, according to

$$a_{r\gamma} = \frac{\mathrm{Re}\{\exp[j(\pi/2)(r + \gamma)]\mathrm{sinc}[k_{zr} + k_{z\gamma} + 2jN_{\mathrm{dz}}] + \exp[j(\pi/2)(r - \gamma)]\mathrm{sinc}[k_{zr} - k_{z\gamma} + 2jN_{\mathrm{dz}}]\}}{[1 + |\mathrm{sinc}(2k_{zr})|][1 + |\mathrm{sinc}(2k_{z\gamma})|]}. \quad (14)$$

Because the sum is symmetric with respect to r and γ, we can add each nondiagonal term, (r, γ), with its complement, (γ, r). These terms are complex conjugates, and all the imaginary parts cancel, leaving

$$s_N(\omega') = \sum_{\substack{p,q,r,\gamma \\ \gamma \le r}} \frac{b_{pqr}b_{pq\gamma}a_{r\gamma}(1 + \delta_{r\gamma})(k_{pqr}^2 k_{pq\gamma}^2 + \omega^2)}{[1 + |\mathrm{sinc}(2k_{xp})|][1 + |\mathrm{sinc}(2k_{yq})|]\{(k_{pqr}^2 k_{pq\gamma}^2 + \omega^2)^2 + (k_{pqr}^2 - k_{pq\gamma}^2)^2\omega^2\}}, \quad (15)$$

where the delta here signifies the Kronecker delta, which is used to account for the diagonal terms $(r = \gamma)$ not having complements.

The PSD expressed in Eq. (15) can be compared with that produced by the use of the Green's function method of analysis. In Elliot *et al.*[9] the noise spectrum for a long detector bar is written in the form

$$S_N(\omega') \propto \frac{\mathrm{sinc}^2(\omega' l_r'/v')}{\left[1 + \left(\frac{D}{\mu^2 E_z^2 \tau}\right)^2 \omega'^2\right]}. \quad (16)$$

The two parts of this can be recognized as a sinc response caused by the finite readout and a single-pole frequency response caused by steady-state diffusion. To obtain a comparable result from the modal PSD of Eq. (15), one must produce an approximate result that has a single-pole response; this implies that we consider only one mode, or one term of the summation.

The first step toward this can be made by the assumption that the top, bottom, and side surfaces are perfectly insulating $(N_{bx} = N_{by} = 0)$. This causes all the p and q terms in the sum to vanish except for $p = q = 0$. This leaves a two-dimensional sum over r and γ. To produce an expression with only one term, we consider only the lowest-order, $r = \gamma = 0$, contribution. Finally, if one assumes that the contact surfaces are perfectly ohmic $(N_{bz} = \infty)$, the PSD becomes

$$S_N(\omega') \propto \frac{1}{[(1 + N_{sx}N_{dz}^2 + N_{sy}\pi^2/4)^2 + \omega'^2]}. \quad (17)$$

Relation (17), which is a modal single-pole response, differs from relation (16) in two important ways. The first is that it lacks the sinc factor caused by the readout. This results from the fact that the modal method incorporates the readout effect by computing a series of modal output weights. These weights are similar to a Fourier decomposition of the readout structure. Because relation (17) uses only one mode, the decomposition has only one term and is insufficient to characterize the readout response. The second difference is that the single-pole response roll-off frequency is given by a more complex, three-term expression in the denominator of relation (17). Each of the terms corresponds to a physical process that reduces the amplitude of any noise perturbation. In this case, the processes are recombination, diffusion interacting with drift, and diffusion interacting with the boundary recombination. The rates of each of these processes are added together to produce the total rate shown. This differs from relation (16), which has only one term because the only process considered there is diffusion interacting with drift. Because the modal theory includes more processes, its relaxation rate

will be faster, and its roll-off frequency will be higher than the Green's function method.

Just as the MTF found by the modal analysis was an infinite sum, so is the PSD. The same considerations as in Ref. 7 concerning accuracy apply here as well: there is computational error, but it can be reduced to an arbitrary level. Our studies showed that the x and y summations converge to less than 0.1% error in approximately ten terms, because of the sinc^2 dependence. The z summation convergence is slower, being driven by the modal wavenumber terms, ${k_{pqr}}^2$, in the denominator. We find that to achieve an accuracy of 1%, we must include terms with an r index to as high as 1500. Although this is less than that required for the MTF calculations, this still involves a fair amount of computation. Because the z sum is two dimensional, running r to 1500 requires more than 840×10^6 terms to be computed.

4. Results and Discussion

The results of Section 3 were evaluated by the use of a computer program. We used a Microsoft FORTRAN compiler on a 486DX2/66 desktop computer. We preserved the accuracy of the sum by using double-precision computations and by evaluating and then summing the terms in an order that tended to keep major cancellation out of the final sum. Approximately 1 h of computation was required to generate a noise PSD curve on this system.

In Fig. 1 we plotted the noise amplitude spectral density (ASD) for a typical SPRITE detector along with the MTF for the same detector, and their ratio. The ASD is simply the square root of the PSD, and it is used here because it is directly comparable with the MTF, and because experimental results are usually given in terms of the ASD (i.e., V/Hz). The noise ASD has been normalized to one at zero frequency. The most interesting feature here is the increase of the noise density at low frequencies. This strongly resembles the observed $1/f$-like behavior of real devices. It is surprising that this is predicted by modal analysis, because none of the usual phenomena associated with $1/f$ noise has been included in the model. This nonuniform frequency distribution results from the transport of charge alone. Each noise carrier exists in the detector for a certain lifetime, which determines the degree of correlation of the noise and thus its spectrum. In simple treatments a single lifetime is assumed, which results in the single-pole response as written in relation (16). In the modal analysis a whole series of lifetimes is used. The long-lived modes correspond to low-frequency fluctuations, and the short-lived modes correspond to high-frequency fluctuations. At low frequency, all the modes of the expansion add together strongly to produce the $1/f$-like behavior. In the midband, the low-frequency modes have cut off, and the remaining high-frequency modes add together in such a way as to produce a flat spectral response. Finally, at high frequencies, all the modes have reached cutoff, and the noise spectrum falls rapidly. Thus, the noise ASD first drops by a fairly large factor, then reaches a constant midband value. Finally, the ASD exhibits its roll-off behavior at a spatial frequency equal to the inverse of the carrier lifetime (not shown in Fig. 1).

By dividing the MTF by the ASD, we obtain the frequency-dependent SNR, which has the property that the maximum SNR occurs not at zero but at some higher frequency. This helps to explain the success of various attempts at using peaking, or boost, filters to flatten the response of SPRITE detectors.[10,11]

The modal approach is useful for predicting the general behavior of the MTF and the PSD, and it allows us to combine the two together as is done in Fig. 1. The resulting frequency-dependent SNR curves can be used to predict trends in device behavior as a function of device parameters.

The effect of the contact boundary conditions is illustrated in Fig. 2. Figure 2 shows the signal-to-noise ratios for a SPRITE in which the contact boundary number has been varied from 0.01 to 100 times the nominal value. This graph tells us something that could not be determined clearly from looking at either the signal or the noise alone. The signal analysis pointed to a contact number of ~0.5 as the optimum value. The noise analysis revealed that the noise is high for a contact number of ten,

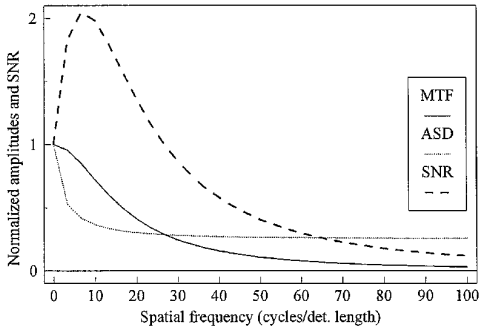

Fig. 1. Comparison of the noise ASD, the signal strength (MTF), and the resulting SNR for a typical detector by use of the eigenmode method.

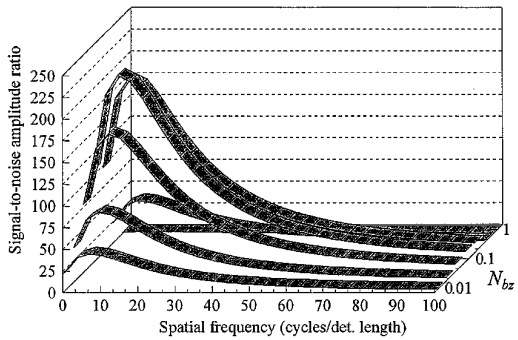

Fig. 2. SNR versus frequency as the detector contact number (N_{bz}) varies from 0.01 to 100 times its nominal value.

and low for values of $N_{bz} > 10$. Both results must be combined to find the true optimum. As can be seen in Fig. 2, the optimum contact number is ~0.5.

The most useful conclusion that we can make from this is that the contact boundary condition is an important factor in determining SPRITE performance. This is not completely surprising, as the issue has been raised for the case of non-SPRITE photoconductive detectors.[12] Because a finite optimum value of surface recombination velocity exists, this property must be controlled if maximum performance is to be expected. One possible method of surface velocity control would be to dope the contacting surface n^+, which causes a potential barrier that slows the recombination of minority carriers; the width and height of the barrier can be controlled in part by adjustment of the penetration and concentration of the dopant. The surface velocity could also be modified through the use of different metals to fabricate the contact. In this case, the use of metals with different work functions will induce recombination barriers of differing heights, thus affecting the surface velocity. Regardless of what method is used, proper control of the contact boundaries promises a large improvement in detector performance.

The effect of the top, bottom, and side boundary conditions were also studied by computation of the modal SNR as N_{bx} and N_{by} were varied from 0.01 to 100 times nominal value. The SNR remains at its maximum value until the side boundary conditions approach 100 times nominal value, which corresponds to boundary numbers around unity. This indicates that the top, bottom, and side boundary conditions should be made as insulating as possible, but that efforts to reduce the boundary numbers below 0.1 are unnecessary.

The influence of the width of the detector was also studied for a range of spreading number, N_{sx}, from 0.01 to 100 times its nominal value. The width spreading parameter[8] is inversely proportional to the square of the width, and so this range corresponds to a range of widths from 0.1 to 10 times nominal. No appreciable change in the SNR with spreading parameter was detected.

5. Conclusions

An analytic form for the noise spectrum of SPRITE detectors has been derived by the use of modal analysis of the charge transport. This derivation included the effects of boundary electrical properties. The modal noise ASD was combined with the modal MTF to produce the spatial frequency-dependent SNR. The effects of the detector boundary electrical properties were investigated by use of the SNR as a means to detect performance trends. The most notable result is that the optimum contact condition is partially blocking, with a boundary number, N_{bz}, of ~0.5. Optimization of the contact in this way holds a potential tenfold increase in the SNR.

This research was supported by Westinghouse Electric Corporation, Orlando, Florida.

References

1. C. T. Elliot, "New detector for thermal imaging systems," Electron. Lett. **17,** 312–313 (1981).
2. D. J. Day and T. J. Shepherd, "Transport in photoconductors—I," Solid-State Electron. **25,** 707–712 (1982).
3. T. J. Shepherd and D. J. Day, "Transport in photoconductors—II," Solid-State Electron. **25,** 713–718 (1982).
4. G. D. Boreman and A. E. Plogstedt, "Modulation transfer function and number of equivalent elements for SPRITE detectors," Appl. Opt. **27,** 4331–4335 (1988).
5. S. P. Braim and A. P. Campbell, "TED (SPRITE) detector MTF," IEE Conf. Publ. **228,** 63–66 (1983).
6. S. P. Braim, "The measurement and analysis of the noise frequency spectrum for SPRITE infrared detectors," in *Infrared Technology and Applications,* L. R. Baker and A. Masson, eds., Proc. Soc. Photo-Opt. Instrum. Eng. **590,** 164–171 (1985).
7. F. J. Effenberger and G. D. Boreman, "Modal analysis of transport processes in SPRITE detectors," Appl. Opt. **34,** 4651–4661 (1995).
8. A. Van der Ziel, *Fluctuation Phenomena in Semi-Conductors* (Academic, New York, 1959), pp. 33–36.
9. C. T. Elliot, D. Day, and D. J. Wilson, "An integrating detector for serial scan thermal imaging," Infrared Phys. **22,** 31–42 (1982).
10. P. Fredin, "Optimum choice of anamorphic ratio and boost filter parameters for a SPRITE based IR sensor," in *Infrared Imaging Systems: Design, Analysis, Modeling and Testing II,* G. C. Holst, ed., Proc. Soc. Photo-Opt. Instrum. Eng. **1488,** 432–442 (1991).
11. P. Fredin and G. D. Boreman, "Resolution-equivalent D^* for SPRITE detectors," Appl. Opt. **34,** 7179–7182 (1995).
12. A. Józwikowska, K. Józwikowski, and A. Rogalski, "Performance of mercury cadmium telluride photoconductive devices," Infrared Phys. **31,** 543–554 (1991).